

Co-ordination of the Crown Thioether 2,5,8-Trithia[9]-*o*-benzenophane (L^1). Synthesis and Crystal Structures of $[CuL^1(Cl)]$ and $[NiL^1_2][BF_4]_2$ †

Lluís Escriche,^{*,a} María-Pilar Almajano,^a Jaume Casabó,^a Francesc Teixidor,^{*,b} Jordi Rius,^b Carlos Miravittles,^b Raikko Kivekäs and Reijo Sillampää^d

^a Departament de Química, Universitat Autònoma de Barcelona, 08193 Bellaterra, Barcelona, Spain

^b Institut de Ciència dels Materials (C.S.I.C.), Campus de Bellaterra, 08193 Bellaterra, Barcelona, Spain

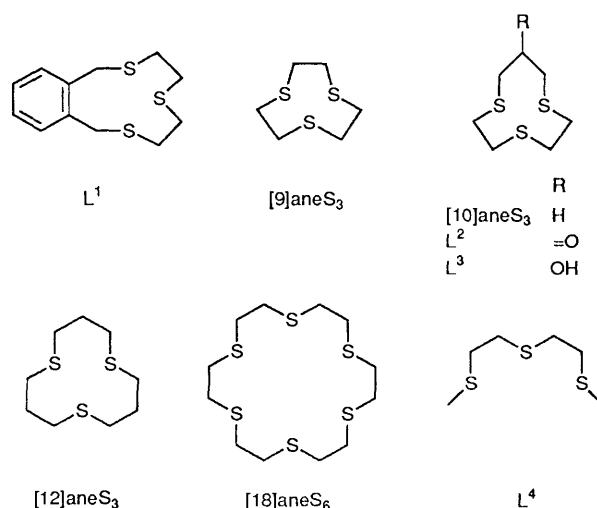
^c Division of Inorganic Chemistry, University of Helsinki, Vuorikatu 20, SF-00100 Helsinki 10, Finland

^d Department of Chemistry, University of Turku, SF-20500 Turku, Finland

The co-ordination abilities of 2,5,8-trithia[9]-*o*-benzenophane (L^1) are compared with several S_3 -crown macrocycles by structural, spectral and electrochemical techniques. Ligand L^1 shows intermediate behaviour relative to the well known ligands 1,4,7-trithiacyclononane and 1,5,9-trithiacyclododecane. The synthesis and characterization of Cu^II , Cu^I , Ni^{II} and Co^{II} complexes with L^1 are carried out. Crystal and molecular structures of two complexes are determined: $[CuL^1(Cl)]$, monoclinic, space group $P2_1/a$, $a = 13.562(6)$, $b = 8.046(1)$, $c = 13.770(6)$ Å, $\beta = 109.96(2)^\circ$, $Z = 4$, $R = 0.041$ and $R' = 0.045$; $[NiL^1_2][BF_4]_2$, monoclinic, space group $P2_1/c$, $a = 9.430(2)$, $b = 14.879(2)$, $c = 11.451(2)$ Å, $\beta = 113.59(1)^\circ$, $Z = 2$, $R = 0.058$ and $R' = 0.057$.

Our purpose is to inquire into the chemical recognition aspect of macrocyclic compounds towards metal ions using them as sensors in membrane-based ion-selective electrodes.¹ In the course of our investigations on polythiamacrocycles incorporating phenyl groups we have studied the closely related compounds 6-oxa-3,9-dithiabicyclo[9.3.1]pentadeca-1(15),-11,13-triene,² 3,6,9-trithiabicyclo[9.3.1]pentadeca-1(15),11,13-triene³ and 3,9-dithiabicyclo[9.3.1]pentadeca-1(15),11,13-triene.³ All are good selective Ag^+ -sensors in membrane-based ion-selective electrodes. It is necessary to find different ligand systems other than these to recognize other metal cations. We have decided to maintain the macrocyclic and polythia character of the ligands, since the co-ordinating properties of the crown thioethers provide a good discrimination between main-group A metal ions and transition-metal ions.

Among crown thioethers, 1,4,7-trithiacyclononane ($[9]aneS_3$) is unique for the remarkable strength and breadth of its complexing ability.⁴ The strong ligating ability of $[9]aneS_3$ derives from its unique conformational suitability for co-ordination.⁵ However, our experience indicates that a strongly co-ordinating ligand is not necessarily a good selective sensor when implemented in membrane-based ion-selective electrodes.⁶ Recently, the synthesis of the closely related molecule 2,5,8-trithia[9]-*o*-benzenophane, L^1 , and some complexes with Mo, Cu, Pd and Ag have been reported.⁷ The molecular structure of the free ligand displays an all-exodentate conformation of the sulfurs, but the ligand easily reorganizes into an endodentate conformation upon metal complexation.^{7b} Molecular dynamics studies on this ligand confirm that there are several exodentate conformations in equilibrium with a short life-time all-endodentate conformation.⁸ For this reason, it is expected to be a mild ligand in the crown- S_3 ligand family. In this paper we compare the co-ordination capabilities of L^1 with respect to the crown- S_3 molecules, $[9]aneS_3$, 1,4,7-trithiacyclododecane ($[10]aneS_3$), 1,5,9-trithiacyclododecane ($[12]aneS_3$),



9-oxo-1,4,7-trithiacyclododecane (L^2) and 9-hydroxy-1,4,7-trithiacyclododecane (L^3). Our aim in the future is to test the sensor capabilities of 2,5,8-trithia[9]-*o*-benzenophane.

Experimental

α, α' -Dichloro-*o*-xylene and 1,5-dimercapto-3-thiapentane were purchased from Aldrich and used as received. All reactions were conducted under a dinitrogen atmosphere using standard Schlenk techniques. All solvents were degassed prior to use. Proton and $^{13}C\{-^1H\}$ NMR spectra were recorded on a Bruker 400 MHz AM instrument. Elemental analysis was performed in our microanalytical laboratory on a Perkin Elmer 240-B instrument.

Cyclic voltammetric measurements were performed under dry dinitrogen atmosphere on 1 mmol dm^{-3} solutions of the complexes in dry nitromethane or acetonitrile containing 0.1 mol dm^{-3} NBu_4PF_6 as a supporting electrolyte, at a rate of

† Supplementary data available: see Instructions for Authors, *J. Chem. Soc., Dalton Trans.*, 1993, Issue 1, pp. xxiii–xxviii.

Table 1 Crystallographic data for $[\text{NiL}^1_2][\text{BF}_4]_2$ and $[\text{CuL}^1(\text{Cl})]^a$

Formula	$\text{C}_{24}\text{H}_{32}\text{B}_2\text{F}_8\text{NiS}_6$	$\text{C}_{12}\text{H}_{16}\text{ClCuS}_6$
Space group	$P2_1/c$	$P2_1/a$ (no. 14)
M	745.18	355.44
$a/\text{\AA}$	9.430(2)	13.562(6)
$b/\text{\AA}$	14.879(2)	8.046(1)
$c/\text{\AA}$	11.451(2)	13.770(6)
$\beta/^\circ$	113.59(1)	109.96(2)
$U/\text{\AA}^3$	1472	1412
Z	2	4
$D_c/\text{g cm}^{-3}$	1.681	1.670
μ/cm^{-1}	11.36	21.4
S^b	1.67	1.53
$R(F_o)^c$	0.058	0.041
$R'(F_o)^d$	0.057	0.045

^a Details in common: monoclinic, Mo-K α radiation ($\lambda = 0.71069$), 293 K. ^b $S = [\sum w(|F_o| - |F_c|)^2 / (n - p)]^{1/2}$ where n is the number of observations and p is the number of parameters. ^c $R = \sum |F_o| - |F_c| / \sum |F_o|$. ^d $R' = [\sum w(|F_o| - |F_c|)^2 / \sum w F_o^2]^{1/2}$.

20–100 mV s⁻¹. A glassy carbon button working electrode and platinum wire counter electrode were used with a Ag–AgCl (KCl 3 mol dm⁻³) electrode as reference. A DACFAMOV 0.510 CNRS-Microtec apparatus, equipped with an Apple IIe microcomputer was used.

UV/VIS spectra were run on a Kontron UVICON 860 and the near-IR spectra on a NIR System 6500 instrument. Magnetic measurements were done on SQUID Quantum-Design equipment from room temperature down to 5 K at 5.5 T.

Synthesis.—2,5,8-Trithia[9]-*o*-benzenophane. This compound was synthesized as previously reported.⁷

Dichloro(2,5,8-trithia[9]-*o*-benzenophane)copper(II). To a solution of $\text{CuCl}_2 \cdot 2\text{H}_2\text{O}$ (0.066 g, 0.387 mmol) in dry tetrahydrofuran (thf) (150 cm³) was added 2,5,8-trithia[9]-*o*-benzenophane (0.125 mg, 0.488 mmol) dissolved in thf (4 cm³). A green precipitate appeared which was filtered off, washed with thf and vacuum dried. Yield: 0.169 g, 88.6% (Found: C, 37.25; H, 4.15. $\text{C}_{12}\text{H}_{16}\text{Cl}_2\text{CuS}_3$ requires C, 36.85; H, 4.10%).

Chloro(2,5,8-trithia[9]-*o*-benzenophane)copper(I). Dichloro(2,5,8-trithia[9]-*o*-benzenophane)copper(II) (0.1 g) was dissolved in methanol (50 cm³) and refluxed for 48 h. The initial green solution became colourless indicating reduction of Cu^{II} to Cu^I. By slow evaporation of the solution a white crystalline precipitate appears affording single crystals suitable for X-ray analysis. Yield: 0.02 g, 20% (Found: C, 40.70; H, 4.40. $\text{C}_{12}\text{H}_{16}\text{ClCuS}_3$ requires C, 40.55; H, 4.50%).

Bis(2,5,8-trithia[9]-*o*-benzenophane)nickel(II) tetrafluoroborate. To a solution of $\text{Ni}(\text{BF}_4)_2 \cdot 6\text{H}_2\text{O}$ (0.131 g, 0.384 mmol) in nitromethane–acetic anhydride (6:1, 5 cm³), was added dropwise a solution of L^1 (0.3 g, 1.17 mmol) in the same solvent (5 cm³). The solution changed from pale green to violet. After 24 h a crystalline material appeared which was suitable for X-ray analysis. The mother-liquor was concentrated and further non-crystalline solid precipitated which was filtered off, washed with nitromethane and acetone and vacuum dried. Yield: 0.15 g, 52% (Found: C, 38.15; H, 4.0. $\text{C}_{24}\text{H}_{32}\text{B}_2\text{F}_8\text{NiS}_6$ requires C, 38.65; H, 4.30%).

Bis(2,5,8-trithia[9]-*o*-benzenophane)cobalt(II) tetrafluoroborate. To a solution of $\text{Co}(\text{BF}_4)_2 \cdot 6\text{H}_2\text{O}$ (0.038 g, 0.11 mmol) in ethanol (1 cm³), was added dropwise a solution of L^1 (0.07 g, 0.27 mmol) in the same solvent. The pink solid which precipitated was filtered off, washed with nitromethane and acetone and vacuum dried. Yield: 0.063 g, 62% (Found: C, 38.60; H, 4.30. $\text{C}_{24}\text{H}_{32}\text{B}_2\text{CoF}_8\text{S}_6$ requires C, 38.65; H, 4.30%).

X-Ray Diffraction Data Collection, Solution and Refinement.—Chloro(2,5,8-trithia[9]-*o*-benzenophane)copper(I). The unit-cell parameters were determined from 25 carefully centred

high-angle reflections ($7 < 2\theta < 21^\circ$) at 293 K on an Enraf Nonius CAD4 (four-circle diffractometer). Crystal data and data collection parameters are summarized in Table 1. 2081 Independent reflections with $\theta \leq 23.5^\circ$ were measured of which 1406 were observed with $I > 2.5\sigma(I)$. Reflections were measured in the range $14 \leq h \leq 14$, $0 \leq k \leq 8$, $0 \leq l \leq 15$. No significant decay of standard reflection intensities was observed (0.8%). The data were corrected for Lorentz and polarization effects and for absorption (transmission coefficients: 0.92–1.00) using the DIFABS program.⁹

The structure was solved by multiresolution direct methods with the Ω tangent formula.¹⁰ All refinements were carried out by the least-squares full-matrix method.¹¹ The hydrogen atoms were introduced in calculated positions and held fixed with two global isotropic thermal parameters (one for hydrogen atoms bonded to $\text{sp}^2\text{-C}$, $U = 0.07$, and one for hydrogen atoms bonded to $\text{sp}^3\text{-C}$, $U = 0.09 \text{ \AA}^2$). The final R and R' values are 0.041 and 0.045 respectively with $w = 1/[\sigma^2(F) + 0.0029F^2]$. Maximum and minimum heights in the final Fourier difference map were 0.25 and -0.30 e \AA^{-3} . Scattering factors were taken from ref. 12.

Bis(2,5,8-trithia[9]-*o*-benzenophane)nickel(II) tetrafluoroborate. The unit-cell parameters were determined by least-squares refinement from 24 carefully centred high-angle reflections ($31 < 2\theta < 40^\circ$) measured at 293 K on a Rigaku AFC5S diffractometer. Crystal data and data collection parameters are summarized in Table 1. 2866 Independent reflections with $\theta \leq 25^\circ$ were measured of which 2713 were observed with $I > 1.00\sigma(I)$. Reflections were measured in the range $-14 \leq h \leq 14$, $0 \leq k \leq 8$, $0 \leq l \leq 15$. The data were corrected for Lorentz and polarization effects, and for absorption (transmission coefficients: 0.92–1.00). Intensity variation of three check reflections was negligible during the data collection.

The structure was solved by direct methods using MITRIL¹³ and DIRDIF¹⁴ programs and subsequent Fourier synthesis. Least-squares refinements minimized the function $\sum w(|F_o| - |F_c|)^2$, [$w = 4F_o^2/\sigma^2(F_o^2)$]. The neutral atom scattering and dispersion factors were taken from ref. 12. After refinement of all non-hydrogen atoms with anisotropic thermal parameters, the hydrogen atoms were found from subsequent Fourier difference maps. Refinement of all atoms, with anisotropic thermal parameters for the non-hydrogen atoms, reduced the R value to 0.058 ($R' = 0.057$). Maximum and minimum heights in the final Fourier difference map were 0.84 and -0.58 e \AA^{-3} . All calculations were performed using the TEXSAN¹⁵ crystallographic software package.

Additional material available from the Cambridge Crystallographic Data Centre comprises H-atom coordinates, thermal parameters and remaining bond lengths and angles.

Results and Discussion

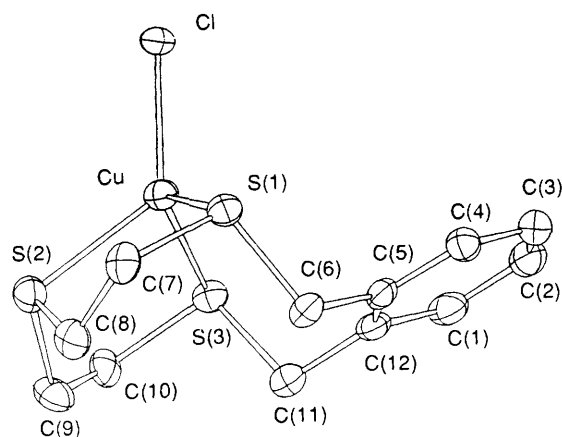
Structural Results.—**Molecular structure of chloro(2,5,8-trithia[9]-*o*-benzenophane)copper(I), $[\text{CuL}^1(\text{Cl})]$.** The unit cell contains four molecules. Fig. 1 shows a perspective view of the molecule with the atom numbering scheme. Final positional parameters for non-hydrogen atoms and selected bond lengths and angles are reported in Tables 2 and 3, respectively.

The copper atom is in a distorted tetrahedral environment provided by the three sulfur atoms of the ligand and one chlorine atom. The Cu–S distances are 2.311(2), 2.398(2) and 2.303(2) Å. The longest Cu–S distance is from the central sulfur atom S(2), as is also found in the molybdenum–carbonyl, copper–phosphine and silver–phosphine complexes with this ligand.^{7a,b} In a similar fashion, the S(1)–Cu–S(3) angle involving the *o*-xylyl fragment [118.6(1)°] is larger than the other two angles [S(1)–Cu–S(2) and S(2)–Cu–S(3)].

The molecular structure of the copper(I) complex is very similar to that observed in $[\text{Cu}(\text{9}]\text{janeS}_3)\text{I}$.¹⁶ Both compounds have the copper(I) ion in a tetrahedral environment provided by three sulfur atoms of the ligand and one co-ordinated halide ion.

Table 2 Final positional parameters with estimated standard deviations (e.s.d.s) in parentheses for the non-hydrogen atoms of [CuL¹(Cl)]

Atom	X/a	Y/b	Z/c
Cu	0.5624(1)	0.0868(1)	0.7085(1)
Cl	0.7222(1)	-0.0043(2)	0.7172(1)
S(1)	0.5209(1)	0.3252(2)	0.6092(1)
S(2)	0.3959(1)	-0.0380(3)	0.6170(1)
S(3)	0.5290(1)	0.0793(2)	0.8616(1)
C(1)	0.6085(5)	0.4585(10)	0.9653(6)
C(2)	0.6802(6)	0.5869(10)	0.9745(7)
C(3)	0.6794(6)	0.6736(10)	0.8893(6)
C(4)	0.6089(5)	0.6353(9)	0.7931(5)
C(5)	0.5360(5)	0.5071(9)	0.7804(5)
C(6)	0.4608(5)	0.4728(9)	0.6736(5)
C(7)	0.4037(6)	0.2508(10)	0.5064(5)
C(8)	0.3306(5)	0.1441(10)	0.5446(5)
C(9)	0.3403(5)	-0.0469(11)	0.7200(6)
C(10)	0.4204(5)	-0.0661(9)	0.8275(5)
C(11)	0.4608(5)	0.2750(9)	0.8623(6)
C(12)	0.5359(5)	0.4165(9)	0.8623(6)

**Fig. 1** ORTEP drawing of the complex [CuL¹(Cl)] showing the atom-numbering scheme. Hydrogen atoms are omitted for clarity; thermal ellipsoids are drawn at the 50% probability level

This is in contrast with the polynuclear structures containing crown thioether bridges found in the copper(I) complex [Cu₂([9]aneS₃)₃][BF₄]₂·H₂O,¹⁷ and in the silver(I) complex [{Ag₃([9]aneS₃)₃}{Ag([9]aneS₃)₂}] [ClO₄]₄.¹⁶ This different behaviour can be explained since non-co-ordinating anions were employed in the synthesis of the latter compounds, while co-ordinating halide ions were used here. Also, owing to steric hindrance in L¹, formation of thioether bridges is not favoured as pointed out by Loeb *et al.*^{7b}

Molecular structure of bis(2,5,8-trithia[9]-o-benzenophane)-nickel(II) tetrafluoroborate, [NiL¹₂][BF₄]₂. The crystal structure of [NiL¹₂][BF₄]₂ consists of discrete [NiL¹₂]²⁺ cations and BF₄⁻ anions. Fig. 2 shows the molecular geometry and the atomic labelling scheme for [NiL¹₂]²⁺. Final positional parameters for non-hydrogen atoms and selected bond lengths and angles are reported in Tables 4 and 5, respectively.

The metal atom occupies a crystallographic inversion centre in a distorted octahedral environment of six sulfur atoms provided by the two facially co-ordinating tridentate thioether ligands. The three Ni-S distances are not identical. The Ni-S(1) and Ni-S(3) distances (2.452, 2.434 Å) are larger than the Ni-S(2) distance (2.387 Å). This introduces a compressed tetragonal distortion in the co-ordination polyhedron around the metal ion. The same kind of distortion is found in [Ni([12]aneS₃)₂]²⁺¹⁸ and [NiL²₂]²⁺,¹⁹ whereas in [Ni([9]aneS₃)₂]²⁺ the geometry is elongated octahedral.²⁰

Both Ni-S(1) and Ni-S(3) distances conform closely to

Table 3 Bond lengths (Å) and angles (°) with e.s.d.s in parentheses for [CuL¹(Cl)]

Cl-Cu	2.252(2)	S(1)-Cu	2.311(2)
S(2)-Cu	2.398(2)	S(3)-Cu	2.303(2)
C(6)-S(1)	1.931(7)	C(7)-S(1)	1.831(6)
C(8)-S(2)	1.822(7)	C(9)-S(2)	1.821(7)
C(10)-S(3)	1.813(6)	C(11)-S(3)	1.828(7)
C(2)-C(1)	1.394(11)	C(12)-C(1)	1.410(10)
C(3)-C(2)	1.361(11)	C(4)-C(3)	1.378(10)
C(5)-C(4)	1.397(10)	C(6)-C(5)	1.502(9)
C(12)-C(5)	1.405(9)	C(8)-C(7)	1.534(10)
C(10)-C(9)	1.515(10)	C(12)-C(11)	1.513(10)
S(1)-Cu-Cl	109.7(1)	S(2)-Cu-Cl	127.5(1)
S(3)-Cu-Cl	115.4(1)	S(2)-Cu-S(1)	92.4(1)
S(3)-Cu-S(1)	118.6(1)	S(3)-Cu-S(2)	91.5(1)
C(6)-S(1)-Cu	108.1(2)	C(7)-S(1)-Cu	99.1(2)
C(7)-S(1)-C(6)	100.0(3)	C(8)-S(2)-Cu	98.4(2)
C(9)-S(2)-Cu	100.0(2)	C(9)-S(2)-C(8)	101.8(4)
C(10)-S(3)-Cu	100.1(2)	C(11)-S(3)-Cu	103.9(2)
C(11)-S(3)-C(10)	100.9(2)	C(12)-C(1)-C(2)	120.1(7)
C(3)-C(2)-C(1)	120.1(7)	C(4)-C(3)-C(2)	120.8(7)
C(5)-C(4)-C(3)	121.0(7)	C(6)-C(5)-C(4)	118.2(6)
C(12)-C(5)-C(4)	118.9(6)	C(12)-C(5)-C(6)	122.9(6)
C(5)-C(6)-S(1)	109.1(4)	C(8)-C(7)-S(1)	114.2(4)
C(7)-C(8)-S(2)	112.8(5)	C(10)-C(9)-S(2)	114.6(5)
C(9)-C(10)-S(3)	115.8(5)	C(12)-C(11)-S(3)	108.4(4)
C(5)-C(12)-C(1)	119.1(6)	C(11)-C(12)-C(1)	117.7(6)
C(11)-C(12)-C(5)	123.1(6)		

Table 4 Final positional parameters with e.s.d.s in parentheses for the non-hydrogen atoms of [NiL¹₂][BF₄]₂

Atom	x	y	z
Ni	0	0	0
S(1)	-0.1381(2)	-0.0988(1)	-0.1816(2)
S(2)	-0.2474(2)	0.0302(1)	0.0024(2)
S(3)	-0.0206(2)	0.1439(1)	-0.1067(2)
F(1)	0.4088(8)	0.2608(4)	-0.0764(6)
F(2)	0.427(1)	0.2891(4)	0.1121(8)
F(3)	0.5428(6)	0.3799(4)	0.0348(6)
F(4)	0.6255(7)	0.2367(4)	0.0959(6)
C(1)	-0.0110(8)	-0.0210(5)	-0.3327(6)
C(2)	0.0350(8)	0.0690(5)	-0.3036(6)
C(3)	0.178(1)	0.0956(6)	-0.3016(7)
C(4)	0.271(1)	0.0358(7)	-0.3293(8)
C(5)	0.225(1)	-0.0523(7)	-0.3580(8)
C(6)	0.087(1)	-0.0798(6)	-0.3578(7)
C(7)	-0.163(1)	-0.0556(6)	-0.3373(7)
C(8)	-0.3378(8)	-0.0994(6)	-0.1948(8)
C(9)	-0.3535(9)	-0.0698(5)	-0.0742(7)
C(10)	-0.3204(9)	0.1138(5)	-0.1238(8)
C(11)	-0.200(1)	0.1852(5)	-0.1024(8)
C(12)	-0.067(1)	0.1359(6)	-0.2776(7)
B	0.506(1)	0.2922(7)	0.0365(9)

the sum of ionic radii of Ni and S (2.44 Å)²¹ as for [Ni([12]aneS₃)₂]²⁺, however the Ni-S(2) distance is shorter and similar to that found in [Ni([9]aneS₃)₂]²⁺. The complex [NiL²₂]²⁺ exhibits similar stereochemical behaviour, but in this case the longest distances are smaller than in [NiL¹₂]²⁺.

The three S-Ni-S bond angles in the chelating unit differ (Table 5) as also found in [NiL²₂]²⁺. However, the S-Ni-S bond angle of the two propylene-linked sulfur atoms in [NiL²₂]²⁺ (96.9°) is smaller than the S-Ni-S bond angle of the two *o*-xylyl-linked sulfur atoms in [NiL¹₂]²⁺ (101.12°). These different bond angles increase the S...S distance in the complex with L¹ relative to that with L², revealing the larger bite of the 1,6- relative to the 1,5-chelating ring.

Table 6 presents some structural features for nickel complexes of [Ni([9]aneS₃)₂]²⁺, [NiL²₂]²⁺, [NiL¹₂]²⁺ and [Ni([12]aneS₃)₂]²⁺. As can be seen, the average Ni-S bond lengths in the

last two complexes closely conform to the sum of their ionic radii (2.44 Å). The average bond distances increase in the order $[\text{Ni}(\text{[9]aneS}_3)_2]^{2+} < [\text{NiL}^2_2]^{2+} < [\text{NiL}^1_2]^{2+}$. The chelating and non-chelating S–Ni–S bond angles are of interest (Table 6): the values of both these parameters for the complex with L^1 lies in between those of the complexes with $[\text{12]aneS}_3$ and L^2 . These structural features are expected to be reflected in the chemical and spectroscopic properties of $[\text{NiL}^1_2]^{2+}$.

Electronic Spectra.— $[\text{NiL}^1_2][\text{BF}_4]_2$. The electronic spectrum of $[\text{NiL}^1_2]^{2+}$ in acetonitrile solution exhibits three bands

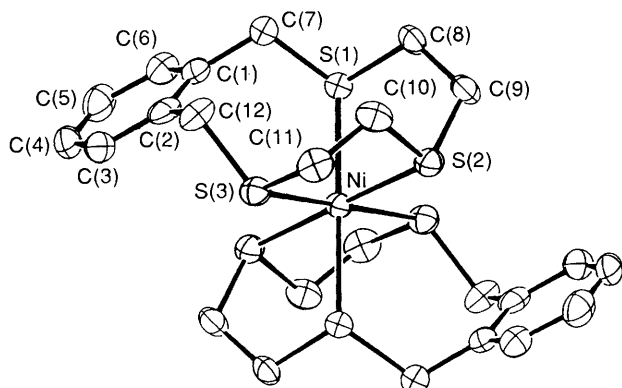


Fig. 2 ORTEP drawing of the cation $[\text{NiL}^1_2]^{2+}$ showing the atom numbering scheme. Hydrogen atoms are omitted for clarity; thermal ellipsoids are drawn at the 50% probability level

Table 5 Selected bond lengths (Å) and angles (°) with e.s.d.s in parentheses for $[\text{NiL}^1_2][\text{BF}_4]_2$

Ni–S(1)	2.452(2)	Ni–S(2)	2.387(2)
Ni–S(3)	2.434(2)	S(1)–C(7)	1.820(8)
S(1)–C(8)	1.828(7)	S(2)–C(9)	1.811(8)
S(2)–C(10)	1.820(8)	S(3)–C(11)	1.821(8)
S(3)–C(12)	1.830(8)	C(1)–C(2)	1.41(1)
C(1)–C(6)	1.38(1)	C(1)–C(7)	1.50(1)
C(2)–C(3)	1.40(1)	C(2)–C(12)	1.49(1)
C(3)–C(4)	1.37(1)	C(4)–C(5)	1.38(1)
C(5)–C(6)	1.37(1)	C(8)–C(9)	1.51(1)
C(10)–C(11)	1.50(1)	F(1)–B	1.34(1)
F(2)–B	1.36(1)	F(3)–B	1.35(1)
F(4)–B	1.34(1)		
S(1)–Ni–S(3)	101.12(6)	S(1)–Ni–S(2)	85.15(6)
Ni–S(1)–C(7)	115.8(3)	S(2)–Ni–S(3)	87.60(6)
C(7)–S(1)–C(8)	101.5(4)	Ni–S(1)–C(8)	104.7(2)
Ni–S(2)–C(10)	100.4(3)	Ni–S(2)–C(9)	101.1(3)
Ni–S(3)–C(11)	99.9(3)	C(9)–S(2)–C(10)	102.5(4)
C(11)–S(3)–C(12)	102.9(4)	Ni–S(3)–C(12)	114.6(3)
C(2)–C(1)–C(7)	122.3(7)	C(2)–C(1)–C(6)	118.8(7)
C(1)–C(2)–C(3)	118.5(7)	C(6)–C(1)–C(7)	118.9(7)
C(3)–C(2)–C(12)	120.2(8)	C(1)–C(2)–C(12)	121.3(7)
C(3)–C(4)–C(5)	120.7(8)	C(2)–C(3)–C(4)	120.8(8)
C(1)–C(6)–C(5)	121.9(8)	C(4)–C(5)–C(6)	119.2(8)
S(1)–C(8)–C(9)	113.4(5)	S(1)–C(7)–C(1)	110.0(5)
S(2)–C(10)–C(11)	109.5(5)	S(2)–C(9)–C(8)	116.4(5)
S(3)–C(12)–C(2)	111.0(5)	S(3)–C(11)–C(10)	114.0(5)

Table 6 Selected structural parameters for nickel(II) complexes of S_3 -crown macrocycles

Complex cation	Average S–Ni bond distance (Å)	Average chelating S–Ni–S bond angle (°)	Average non-chelating S–Ni–S bond angle (°)	Ref.
$[\text{Ni}(\text{[9]aneS}_3)_2]^{2+}$	2.386	88.5	91.5	19
$[\text{NiL}^2_2]^{2+}$	2.409	89.0	88.9	22
$[\text{NiL}^1_2]^{2+}$	2.424	91.6	88.4	This work
$[\text{Ni}(\text{[12]aneS}_3)_2]^{2+}$	2.422	94.2	85.8	17

at 864 ($\epsilon = 22$), 557 ($\epsilon = 33$) and 395 nm ($\epsilon = 364 \text{ dm}^3 \text{ mol}^{-1} \text{ cm}^{-1}$). The first two absorptions are assigned to the d–d transitions ${}^3\text{A}_{2g} \rightarrow {}^3\text{T}_{2g}$ and ${}^3\text{A}_{2g} \rightarrow {}^3\text{T}_{1g}(\text{F})$ respectively, characteristic of a Ni^{2+} ion in an octahedral environment, while the highest energy absorption is assigned to a charge-transfer band overlapping with the third allowed d–d transition of a d^8 ion in an octahedral co-ordination [${}^3\text{A}_{2g} \rightarrow {}^3\text{T}_{1g}(\text{P})$]. Table 7 reports the electronic spectra and calculated crystal-field parameters for several nickel(II) complexes with trithia ligands in acetonitrile. Ligand L^1 exerts a crystal-field strength lower than $[\text{9]aneS}_3$, $[\text{10]aneS}_3$ and L^2 , but higher than those of L^3 and $[\text{12]aneS}_3$. In this series of nickel(II) complexes, the crystal-field strength (as measured by the Δ_o parameter) is probably in the order: $[\text{9]aneS}_3 > [\text{10]aneS}_3 > \text{L}^2 > \text{L}^1 > \text{L}^3 > [\text{12]aneS}_3$. The β crystal-field parameter is correlated with metal–ligand orbital overlap,^{18,24,25} depending on the β value, these ligands can be broadly classified into two groups according to their ability to co-ordinate to Ni^{II} . The ligands $[\text{9}]$ - and $[\text{10]aneS}_3$ exhibit lower β values, and so co-ordinate strongly, while L^1 , L^2 , $[\text{12]aneS}_3$ and L^3 , which display similar and higher β values, are poorer co-ordinating ligands.

$[\text{CoL}^1_2][\text{BF}_4]_2$. The electronic spectrum of $[\text{CoL}^1_2]^{2+}$ in nitromethane solution exhibits three absorption bands at 812 ($\epsilon = 12$), 486 ($\epsilon = 108$) and 388 nm ($\epsilon = 7100 \text{ dm}^3 \text{ mol}^{-1} \text{ s}^{-1}$). The two first bands are assigned to d–d transitions, while the higher energy one is a charge-transfer band. Table 7 reports the absorption bands displayed by the $[\text{Co}(\text{[9]aneS}_3)_2]^{2+}$ complex to allow comparison with $[\text{CoL}^1_2]^{2+}$. No reports are found in the literature of the electronic spectrum of $[\text{Co}(\text{[12]aneS}_3)_2]^{2+}$, revealing its instability in solution. No spectra could be obtained for $[\text{CoL}^1_2]^{2+}$ in acetonitrile, solutions turning from pale pink to blue over a few seconds, revealing a rapid change of the cobalt(II) co-ordination sphere.

The electronic spectra of the well known low-spin $[\text{Co}(\text{[9]aneS}_3)_2]^{2+}$ and the corresponding cobalt(II) complex with L^1 show close similarity, despite the absence of absorptions above 500 nm for the $[\text{9]aneS}_3$ complex in nitromethane. There is also a good agreement between both spectra and those exhibited by the low-spin isoelectronic nickel(III) complexes $[\text{Ni}(\text{[9]aneN}_3)]^{3+}$ ($[\text{9]aneN}_3 = 1,4,7\text{-triazacyclononane}$)²⁶ and $[\text{Ni}(\text{dtne})]^{3+}$ [$\text{dtne} = 1,2\text{-bis}(1,4,7\text{-triazacyclonon-1-yl})\text{ethane}$].²⁷ The effective magnetic moment of $[\text{CoL}^1_2][\text{BF}_4]_2$ at room temperature (273.8 K) is 1.89 decreasing to 1.61 μ_B at 5.0 K, values typical for low-spin cobalt(II).²⁸ All these facts allow a low-spin octahedral geometry to be assigned to $[\text{CoL}^1_2]^{2+}$.

Electrochemistry.—The cyclic voltammetry of L^1 in acetonitrile or nitromethane (solvent range -1.1 to $+1.0$ V vs. ferrocene–ferrocenium) shows an irreversible oxidation peak at 0.86 V and a reduction peak at -0.89 V. This behaviour is similar to that displayed by the $[\text{9]aneS}_3$ ($+0.99$ and -0.70 V)²⁴ and several other aliphatic thioethers.²²

The cyclic voltammetry of $[\text{NiL}^1_2]^{2+}$ in acetonitrile solution shows two quasi-reversible waves at $E_{1/2} = -1.03$ V ($i_p = 1.00$) and $E_{1/2} = -0.78$ V ($i_p = 0.60$). On the contrary, in nitromethane only irreversible waves assigned to the organic ligand are observed. Probably the solvent plays a significant role in the electrochemical properties of these complexes. The observed quasi-reversible redox couples in acetonitrile of

Table 7 Electronic spectra and ligand-field parameters for complexes of Ni^{II} and Co^{II} with S₃-crown macrocycles

Complex	λ/nm ($\epsilon/\text{dm}^3 \text{ mol}^{-1} \text{ cm}^{-1}$)	Δ_0/cm^{-1}	β^*	Solvent	Ref.
[Ni([9]aneS ₃) ₂] ²⁺	790 (30), 530 (30)	12 650	0.66	MeCN	17
[Ni([10]aneS ₃) ₂] ²⁺	807 (33), 544 (54)	12 390	0.63	MeCN	22
[NiL ₂] ²⁺	833 (11), 541 (16)	12 000	0.73	MeCN	22
[NiL ₂] ²⁺	864 (22), 557 (33)	11 570	0.74	MeCN	This work
[NiL ₂] ²⁺	877 (30), 562 (30)	11 400	0.75	MeCN	22
[Ni([12]aneS ₃) ₂] ²⁺	890 (25), 570 (34)	11 240	0.74	MeCN	17
[Co([9]aneS ₃) ₂] ²⁺	478 (76), 335 (7000), 262 (7300)			MeNO ₂	23
[Co([9]aneS ₃) ₂] ²⁺	730 (11), 560 (sh), 480 (92), 338 (6600)			MeCN	This work
[CoL ₂] ²⁺	812 (12), 486 (sh, 108), 388 (7100)			MeNO ₂	This work

* $\beta = B_{\text{complex}}/B_{\text{free ion}}$, $B_{\text{free ion}} = 1038 \text{ cm}^{-1}$; $B_{\text{complex}} = (2\gamma_1^2 + \gamma_2^2 - 3\gamma_1\gamma_2)/(15\gamma_2 - 27\gamma_1)$ where $\gamma_1 = \Delta_0$, $\gamma_2 =$ second observed band and B is the Racah Parameter.

[NiL₂]²⁺ are in the same range as the free-ligand reduction peak. It is thus reasonable to assign these two reductions to ligand based processes, modified by co-ordination to the metal.

The instability of [CoL₂]²⁺ in acetonitrile solution ruled out an electrochemical study in this solvent. In nitromethane the voltammogram shows two quasi-reversible waves at $E_{1/2} = +0.31 \text{ V}$ and $E_{1/2} = -0.70 \text{ V}$. As has been suggested for [Co([9]aneS₃)₂]²⁺,²⁸ the first peak is assigned to the Co^{III}-Co^{II} redox couple and the second to Co^{II}-Co^I. This behaviour contrasts with that found for [CoL₂]²⁺ (L⁴ = 2,5,8-trithianonane) and [Co([18]aneS₆)₂]²⁺ ([18]aneS₆ = 1,4,7,10,13,16-hexathiacyclooctadecane), which only exhibit one reversible wave at $E_{1/2} = +0.31$ and $+0.33 \text{ V}$, respectively, assigned to the Co^{III}-Co^{II} redox couple.²⁶

From these data, it can be concluded that L¹ stabilizes Co^{II} better than [9]aneS₃, with respect to Co^{III}. The differences between $E_{1/2}$ (Co^{III}-Co^{II}) values for [9]aneS₃, L⁴ and [18]aneS₆ have been attributed to the superior co-ordinating ability of the first ligand towards Co^{III}.²⁹ The $E_{1/2}$ (Co^{III}-Co^{II}) values for complexes of cobalt(II) with L¹, [18]aneS₆ and L⁴ are very similar. Destabilization of Co^{III} in the L¹ system is probably a consequence of steric or conformational effects of the *o*-xylyl unit so reducing its co-ordination capability.

Cyclic voltammetry of [CuL¹Cl₂] in nitromethane solution reveals an essentially reversible one-electron wave at $+0.12 \text{ V}$. This value is in agreement with that found for similar thioether copper complexes with co-ordinating counter anions.³⁰ These results are not easily comparable with those found for copper(II) complexes of [9]aneS₃ and [18]aneS₆, since for these the anions are non-co-ordinating.³¹

Conclusion

It is interesting to consider the ready reduction of Cu^{II} to Cu^I (at room temperature in methylene chloride, acetonitrile or nitromethane) for [CuL¹Cl₂]. Similar behaviour has been reported for copper(II) complexes with small, acyclic thioethers.³² This fact is also in accord with the preferential stabilization of Co^{II} versus Co^{III} in [CoL₂]²⁺ as revealed by electrochemical studies. By comparison with copper and cobalt complexes of [9]aneS₃, it can be concluded that L¹ stabilizes lower oxidation states relative to [9]aneS₃.

From structural and spectral data of the nickel(II) complexes, L¹ could be considered as intermediate in complexing ability when comparing it with [9]aneS₃, L² and [12]aneS₃. Several authors justify the good co-ordinating capabilities of [9]aneS₃ by its all-endodentate conformation.^{4,17} Probably, this structural feature is due to the presence of SCH₂CH₂S moieties. Replacement of SCH₂CH₂S by SCH₂CH₂CH₂S leads to [12]aneS₃ in which the sulfurs are exodentate and so leads to poorer co-ordinating properties. Replacement of only one SCH₂CH₂S in [9]aneS₃ by SCH₂CR₂CH₂S [R₂ = H₂, =O or H(OH)] gives ligands [10]aneS₃, L² and L³, which display

intermediate co-ordinating capabilities. In L¹, one of the SCH₂CH₂S units in [9]aneS₃ has been replaced by a SCH₂(C₆H₄)CH₂S group, similar to a S(CH₂)₄S moiety, but reinforced by a rigid aromatic benzene ring.

Acknowledgements

This work was partially financed by Comisión Interministerial de Ciencia y Tecnología (CICYT) MAT91-0952 from the Spanish Government.

References

- 1 J. Casabó, L. Escriche, S. Alegret, C. Jaime, F. Teixidor, C. Pérez-Jiménez, L. Mestres, J. Rius, E. Molins and C. Miravittles, *Inorg. Chem.*, 1991, **30**, 1893.
- 2 J. Casabó, C. Pérez-Jiménez, L. Escriche, S. Alegret, E. Martínez-Fábregas and F. Teixidor, *Chem. Lett.*, 1990, 1107.
- 3 J. Casabó, L. Mestres, L. Escriche, F. Teixidor and C. Pérez-Jiménez, *J. Chem. Soc., Dalton Trans.*, 1991, 1969.
- 4 S. R. Cooper, *Acc. Chem. Res.*, 1988, **114**, 1431; A. J. Blake and M. Schröder, *Adv. Inorg. Chem.*, 1990, **35**, 1.
- 5 W. N. Setzer, B. R. Coleman, G. S. Wilson and R. S. Glass, *Tetrahedron*, 1981, **38**, 2743; R. S. Glass, G. S. Wilson and W. N. Setzer, *J. Am. Chem. Soc.*, 1980, **102**, 5068.
- 6 J. Casabó, L. Escriche, M. P. Almajano-Pablos and F. Teixidor, unpublished work.
- 7 (a) B. de Groot and S. J. Loeb, *Inorg. Chem.*, 1990, **29**, 4084; (b) B. de Groot and S. J. Loeb, *J. Chem. Soc., Chem. Commun.*, 1990, 1755; (c) B. de Groot, G. R. Giesbrecht, S. J. Loeb and K. H. Shimiza, *Inorg. Chem.*, 1991, **30**, 177; (d) B. de Groot, G. S. Hannan and S. J. Loeb, *Inorg. Chem.*, 1991, **30**, 4645.
- 8 J. C. Lockhart, D. P. Mousley, M. N. S. Hill, N. P. Tomkinson, F. Teixidor, M. P. Almajano, L. Escriche, J. Casabó, R. Sillanpaa and R. Kivekäs, *J. Chem. Soc., Dalton Trans.*, 1992, 2889.
- 9 N. Walker and D. Stuart, *Acta Crystallogr., Sect. A*, 1983, **39**, 159.
- 10 J. Rius and C. Miravittles, *Acta Crystallogr., Sect. A*, 1989, **45**, 490.
- 11 G. M. Sheldrick, SHELX 76, University of Cambridge, 1976.
- 12 *International Tables for X-Ray Crystallography*, Kynoch Press, Birmingham, 1974, vol. 4 (Present distributor D. Reidel, Dordrecht).
- 13 C. J. Gilmore, *J. Appl. Crystallogr.*, 1984, 42.
- 14 P. T. Beurskens, DIRDIF, Direct methods for difference structures, an automatic procedure for phase extension and refinement of difference structure factors, Technical Report 1984/1, Crystallography Laboratory, Toernooiveldt, Nijmegen, 1984.
- 15 TEXSAN-TEXRAY Structure Analysis Package, Molecular Structure Corporation, Houston, TX, 1985.
- 16 H. J. Küppers, K. Wieghardt, Yi-Hung Tsay, C. Krüger, B. Nuber and J. Weiss, *Angew. Chem., Int. Ed. Engl.*, 1987, **26**, 575.
- 17 J. A. Clarkson, R. Yagbasan, P. J. Blower and S. R. Cooper, *J. Chem. Soc., Chem. Commun.*, 1989, 1244.
- 18 S. R. Cooper, S. C. Rawle, J. R. Hartmon, E. J. Hints and G. A. Adams, *Inorg. Chem.*, 1988, **27**, 1209.
- 19 H. Küppers, A. Neves, C. Pomp, D. Ventur and K. Wieghardt, *Inorg. Chem.*, 1986, **25**, 2400.
- 20 W. N. Setzer, C. A. Ogle, G. S. Wilson and R. S. Glass, *Inorg. Chem.*, 1983, **22**, 226.
- 21 S. G. Murray and F. R. Hartley, *Chem. Rev.*, 1981, **81**, 365.
- 22 J. Q. Chamber, *Encyclopedia of Electrochemistry of the Elements*,

- eds. A. J. Bard and H. Lund, Marcel Dekker, New York, 1978, Organic Section, vol. 12, p. 329; P. T. Cottrell and C. J. K. Mann, *J. Electrochem. Soc.*, 1969, **116**, 1499.
- 23 G. S. Wilson, D. D. Swanson and R. S. Glass, *Inorg. Chem.*, 1986, **25**, 3827.
- 24 K. Wieghardt, H. Küppers and J. Weiss, *Inorg. Chem.*, 1985, **24**, 3067.
- 25 W. N. Setzer, E. L. Cacioppo, G. J. Grant, D. D. Kim, J. L. Hubbard and D. G. Van Derveer, *Inorg. Chem.*, 1990, **29**, 2672.
- 26 K. Wieghardt, W. Schmidt, W. Herrmann and H. Küppers, *Inorg. Chem.*, 1983, **22**, 2953.
- 27 K. Wieghardt, W. Tolksdorf and W. Herrmann, *Inorg. Chem.*, 1985, **24**, 1230.
- 28 J. R. Hartman, E. J. Hintsä and S. R. Cooper, *J. Am. Chem. Soc.*, 1986, **108**, 1208.
- 29 H. J. Küppers, A. Neves, C. Pomp, D. Ventur, K. Wieghardt, B. Nuber and J. Weiss, *Inorg. Chem.*, 1986, **25**, 2400.
- 30 F. Teixidor, G. Sánchez-Castelló, N. Lucena, L. Escriche, R. Kivekäs, R. Sundberg and J. Casabó, *Inorg. Chem.*, 1992, **30**, 4931.
- 31 J. R. Hartman and S. R. Cooper, *J. Am. Chem. Soc.*, 1986, **108**, 1202.
- 32 M. M. Olmstead, W. K. Musker and R. M. Kesler, *Inorg. Chem.*, 1981, **20**, 151.

Received 14th May 1993; Paper 3/02741D